LIQUEFACTION SUSCEPTIBILITY OF THE BAYAMON AND SAN JUAN QUADRANGLES, PUERTO RICO

FINAL TECHNICAL REPORT

Recipient:

William Lettis & Associates, Inc.
1777 Botelho Drive Suite 262, Walnut Creek, CA 94596
Phone: (925) 256-6070 Fax: (925) 256-6076
URL: www.lettis.com

Principal Investigators:

Jeffrey L. Bachhuber, James V. Hengesh, and Sean T. Sundermann
email: bachhuber@lettis.com, email: hengesh@lettis.com

Program Elements I:

Products for Earthquake Loss Reduction

Keywords:

Liquefaction, Regional Seismic Hazard, Site Effects, Puerto Rico

U.S. Geological Survey
National Earthquake Hazards Reduction Program
Award 03HQGR0107

January 2008

This research was supported by the U.S. Geological Survey (USGS), Department of the Interior, under USGS award number 03HQGR0107. The views and conclusions contained in this document are those of the Principal Investigators and should not be interpreted as necessarily representing the official policies, either expressed or implied of the U.S. Government.

Award 03HQGR0107

U.S. Geological Survey
National Earthquake Hazards Reduction Program

LIQUEFACTION SUSCEPTIBILITY OF THE BAYAMON AND SAN JUAN QUADRANGLES, PUERTO RICO

Jeffrey L. Bachhuber, James V. Hengesh and Sean T Sundermann

William Lettis & Associates, Inc.
1777 Botelho Drive Suite 262, Walnut Creek, CA 94596
Phone: (925) 256-6070 Fax: (925) 256-6076
email: bachhuber@lettis.com, email: hengesh@lettis.com

TECHNICAL ABSTRACT

A liquefaction susceptibility map was prepared for the rapidly developing Bayamon area and combined with our previous map that was prepared for the San Juan area (Hengesh and Bachhuber 1999). The map area includes important lifeline corridors, power plants, industrial and pharmaceutical manufacturing facilities.

The liquefaction susceptibility map was developed through a five step process including: (1) preparation of a detailed Quaternary geological map delineating deposits age, depositional environment, and texture; (2) evaluation of Quaternary deposit thickness and depth to groundwater; (3) initial evaluation of relative liquefaction susceptibility (decision tree); (4) liquefaction triggering evaluation using geotechnical borehole data and the Seed and Idriss (1971b) “Simplified Procedure”; and, (5) identification of units of similar susceptibility and the formation of liquefaction susceptibility zones. The map depicts seven liquefaction hazard zones for the San Juan and Bayamon area that range from Very Low Hazard to Very High Hazard.

The areas of highest liquefaction hazard occur along the low-lying coastal plain where beach, river, and swamp sediments interfinger to form relatively thick sequences of loose, fine grained cohesionless deposits. The Rio Bayamon and Rio de la Plata valleys both contain highly susceptible deposits. The areas underlain by Quaternary silica sands, blanket deposits, colluvium, valley fill, and alluvial fan deposits have low to moderate susceptibility to liquefaction. Most of the areas to the south of the coastal plain lie within Moderate, Low, or Very Low hazard zones.

This research directly addresses **Element I (Earthquake Hazards Assessments - Products for Earthquake Loss Reduction)**, which requested research with the goal of assessing *"earthquake hazards and reducing losses in urban areas; and producing and demonstrating products that enable the public and private sectors to assess earthquake hazards and implement effective mitigation strategies"*. Our new combined susceptibility map supports ongoing efforts by various Puerto Rican governmental and earth science organizations. The GIS maps and data map layers produced by this research provide a publicly available information resource to assess ground deformation hazards, develop mitigation measures, and to assess potential risks to critical lifelines and other facilities that support the large population of the greater San Juan area.

TABLE OF CONTENTS

LIST OF TABLES

1.0 INTRODUCTION

Previous investigations of the San Juan, Puerto Rico Quadrangle showed that the area contains geological deposits that have a range of liquefaction susceptibility that varies from very low to very high for earthquakes that are likely to occur in the region (Hengesh and Bachhuber, 1999, 2005). The results of this previous investigation indicated the need to expand the liquefaction hazard mapping to the adjacent Bayamon Quadrangle. The current investigation was completed to map the distribution of these liquefiable deposits in the Bayamon Quadrangle and to combine this mapping with our previous liquefaction map for the San Juan quadrangle (Figure 1).

The combined liquefaction susceptibility map for the Bayamon and San Juan quadrangles depicts the areal distribution and relative hazard from liquefiable deposits across the greater San Juan Puerto Rico area. Development of this map will aid in hazard mitigation and risk reduction efforts in the greater San Juan area, which is the most rapidly growing and densely populated part of Puerto Rico. The project area includes essential airports and port facilities, petrochemical facilities and power plants, government centers and universities, and sensitive pharmaceutical and manufacturing centers. Long reaches of lifeline facilities that support the populations in this region also traverse the study area.

Prior to Puerto Rico's rapid development beginning in the mid-1900's, the northern coastal plain was comprised of alluvial fans, marshes, mangrove swamps, and estuarine channels and lagoons. The northern coastal plain has been undergoing intensive development with broad areas of these low-lying areas being reclaimed through drainage of surface waters and placement of fills. Although development is now progressing across the reclaimed land, these broad, low-lying areas are underlain by a significant thickness (up to 135 feet) of unconsolidated Quaternary deposits. The Quaternary deposits underlying the coastal plain contain interlayered deposits of soft organic-rich clay, silts and fine sands, and discontinuous layers of gravel. Because of the low elevations and proximity to the coast, groundwater across the coastal plain occurs at shallow depth. The distribution of loose, fine grained, cohesionless deposits and shallow groundwater indicates that broad areas of the San Juan and Bayamon quadrangles are susceptible to liquefaction and related ground deformation during future earthquakes that are likely to occur in the region.

The maps developed during this project will assist Puerto Rico in its efforts to characterize and mitigate seismic hazards, reduce risks from these hazards, and plan future development. The previous San Juan maps have been incorporated into the Puerto Rico Planning Board GIS database for governmental use, and are available to the public through this organization (www.jp.gobierno.pr). This new map also will be made available to the Puerto Rico Government for use and distribution to the public.

2.0 REGIONAL SEISMIC SETTING

Puerto Rico lies along the Northern Caribbean Plate Boundary Zone (NCPBZ), a seismically active region characterized by convergence and lateral translation of the North American and Caribbean plates (Mann et al., 2005; Mann et al., 2002; McCann et al., 2002). As shown on Figure 2, the major tectonic elements of the region include the Puerto Rico and Muertos Trough subduction zones (located north and south of the island, respectively), the Anegada and Mona Passages (located east and west of the island, respectively), and segments of the Great Southern Puerto Rico fault zone that cross the island from northwest to southeast (Masson and Scanlon, 1991). Geodetic data for the northeastern Caribbean region indicate an ~20 mm/yr rate of relative motion across the NCPBZ (Mann et al., 2002). Several large-magnitude historical earthquakes demonstrate the seismic potential of the region. Major earthquakes were reported in 1670, 1787, 1867, and 1918 (McCann 1990, 2002, Doser et al., 2005). The May 2, 1787 earthquake on the Puerto Rico subduction zone produced Modified Mercalli Intensities (MMI) of VII to VIII and caused significant damage to the northern part of the island (McCann, et al., 2002). The November 18, 1867 event in the Anegada Passage produced Rossi-Forel (RF) intensity IX in the Virgin Islands, and MMI intensity VIII in eastern Puerto Rico (Reid and Taber, 1919). The October 18, 1918 M7.5 event in Mona Passage produced MMI intensity IX in western Puerto Rico, and was the most destructive earthquake recorded on the island (Reid and Taber, 1919; Doser et al., 2005).

Probabilistic seismic hazard analyses (PSHA) have been conducted for Puerto Rico to estimate the probabilities that certain levels of strong ground shaking might occur during future time intervals (Crouse and Hengesh, 2003; Mueller et al., 2003). The results of the PSHA's for the San Juan area indicate that ground motions with a 10% probability of exceedence in 50 years (approximately 475-year return period) are about 0.25g, and ground motions with a 2% probability of exceedence in 50 years (2475-year return period) are about 0.45g. These two ground motion estimates are well above the triggering threshold values for liquefaction of susceptible deposits in the San Juan area. The historical seismicity and seismotectonic setting of Puerto Rico demonstrate that the opportunity exists to cause liquefaction in susceptible sediments.

3.0 GEOLOGICAL CONDITIONS IN THE SAN JUAN AND BAYAMON AREAS, PUERTO RICO

The urbanized northern coastal plain of Puerto Rico (Figure 3) is underlain by Tertiary limestone (Monroe, 1980) and extensive Quaternary sediments deposited by fluvial, marine, and eolian processes. Most bedrock units are mantled by thick residual clay soils or are deeply weathered saprolite. Quaternary sediments include sands, clayey sands, sand and gravel, soft organic clay, silty clay, peat, and calcareous mud that accumulated in streams, beaches, lagoons, estuaries, and swamps (Figure 2; Monroe, 1968, 1973; Pease and Monroe, 1977). Eolian sands also are deposited along the coastline and increase the sand component of the swamp and estuarine deposits near the beach. Much of the built-up areas of the San Juan and Bayamon quadrangles along lagoon or coastal margins were formed by artificial filling that locally included sluicing of hydraulic fill (Monroe, 1980; Ellis, 1976). The quality and texture of the fill vary greatly across the study area. In general, older fill along the margins of lagoons and bays is sandy hydraulic fill that was sluiced or dumped into place to form broad tracts of reclaimed land. The filling was typically accomplished using sandy material dredged from the lagoons, and was placed mainly before the early 1970's, and in some cases in the late 1800's and early 1900's (Ellis, 1976).

Based on the geological mapping, aerial photograph interpretation, and field reconnaissance the Quaternary geologic history of the greater San Juan metropolitan area involves extensive erosion of material from the highlands and deposition of alluvium and alluvial fan complexes along the stream systems and slopes. These deposits interfinger with coastal lagoonal deposits and beach-eolian sands on the coastal plain. A combination of sea-level change and regional tectonic uplift (Horsfield, 1975; Monroe, 1968; Taggert and Joyce, 1989) has caused Holocene river channels to be incised within broad Pleistocene flood plains. Examples of this process are large Pleistocene alluvial fan complexes that have been incised by Rio Piedras in the Hato Rey District and Rio Bayamon in the eastern Bayamon Quadrangle (Figure 3). Holocene alluvium of major drainage systems were deposited within terraces and floodplains that are incised into the former fan surfaces to depths of approximately 5 to 10 meters. Holocene deposits generally appear confined to the incised channel systems, alluvial fans, beach, estuary, and lagoonal environments.

In addition to regional tectonic uplift, Quaternary sea-level fluctuations have changed stream base levels and have influenced the development of stream systems and deposition of sediment along the northern coastal plain. Coastal streams were incised and graded to lower base levels during low stands of sea level. Paleo-valleys that formed during sea level low stands were drowned and filled as sea level rose to its present elevation through the Holocene. Former beach sands were blown into dunes, and sand sheets that migrated inland stabilized as eolian sand sheets (referred to as the "silica sands"). The bay and estuary deposits of Sabana Seca, Bahia de San Juan and Laguna San Jose and alluvial deposits shed from the coastal mountains now blanket much of the former low-lying landscape (Figure 3). Swamps and mangroves that formed at lower stands of sea level are now preserved as peat layers within the bay and estuary deposits.

4.0 FACTORS INFLUENCING LIQUEFACTION SUSCEPTIBILITY

Liquefaction susceptibility is controlled by a number of factors including grain size distribution (texture), soil density, depth to ground water, and the liquefaction triggering threshold with respect to the level of ground shaking that might be anticipated for a study region (Youd et al., 2001, 2003; Seed et al., 2002). The texture and soil density are strongly controlled by depositional environment and deposit age, which allows application of Quaternary geological mapping principles to define the distribution and areal extent of potential liquefaction susceptibility map units (Youd and Perkins, 1978). Liquefaction is restricted to areas with a narrow range of geologic and hydrologic characteristics that can be identified and mapped based on established Quaternary mapping techniques (Youd and Perkins, 1978).

The depositional environment controls the texture, sorting and packing of sediments (Youd and Perkins, 1978). For example, high-energy environments such as beaches and fast-flowing rivers preferentially sort grains, and result in a coarse grained, densely packed deposit. Low energy environments such as lagoons and estuaries form predominantly fine-grained, loosely packed deposits. Deposits with higher relative densities and more stable soil structure have a lower susceptibility to liquefaction. The amount of clay in a deposit dramatically affects a deposit's susceptibility to liquefaction. In a general sense, cohesive soils that contain more than 10 to 30 percent of plastic clay may be considered nonliquefiable (Seed et al., 2002). For this reason, Quaternary geological mapping can be applied to delineate map units formed in depositional environments characterized by high clay content, or to delineate map units where aging effects have increased the clay content of the deposit (Birkeland, 1984). With increasing age, the relative density of a deposit may increase as particles gradually align and consolidate together and the deposit undergoes long-term drainage. The soil structure also may become more stable with age through particle reorientation or cementation. Additionally, over time, sand and silt grains are reduced in size and undergo mineralogical decomposition to clay by mechanical and chemical weathering (e.g., Mitchell, 1999). These mechanical, mineralogical, and cementation changes in the deposit are permanent effects that become "locked" into the deposit and dramatically reduce their susceptibility to liquefaction. In some cases, older soils have undergone burial and compaction, followed by a period of uplift and erosional unloading. The process of burial and exhumation causes the soils to be in an overconsolidated state, which also greatly reduces their susceptibility to liquefaction (Youd et al., 2001, 2003).

Quaternary geological and geomorphological mapping provides an important first step in assessing liquefaction susceptibility by identifying geologic deposits whose age and textural characteristics are most susceptible to liquefaction. Most liquefaction occurs in areas of poorly engineered hydraulic fills and in late Holocene fluvial deposits (e.g., Pyke, 2003; Youd et al., 2001, 2003). Therefore, our Quaternary and geomorphologic mapping for the San Juan and Bayamon quadrangles concentrated on identification and microzonation (where possible) of artificial fill and latest Holocene deposits. We also estimated the relative age of other Quaternary deposits to form an age-based susceptibility ranking system shown on Figure 4. We use the age of deposits as one criteria to establish the relative liquefaction susceptibility of geologic (Youd and Perkins, 1978; Youd, 1991; Tinsley et al., 1985; Bachhuber et al., 1994; and, Hitchcock et al., 1999). Of critical importance is the differentiation of geological deposits of Holocene and Pleistocene age. In general, historic occurrences of severe liquefaction have been largely or wholly restricted to hydraulic fills and natural alluvial deposits of late Holocene age (e.g., Pyke, 2003; Rathje and others, 2003).

Depth to groundwater is a significant factor governing liquefaction susceptibility. Saturation reduces the normal effective stress acting on loose, sandy sediments. This condition, particularly in the upper 20 meters of the ground surface, increases the likelihood of liquefaction and resulting ground failure (Youd and Perkins, 1978). Because groundwater levels may vary due to seasonal variations and historic groundwater use, we used the highest reasonable water levels for the liquefaction susceptibility analysis.
The level of strong ground shaking anticipated for a study region is an important consideration for specifying liquefaction susceptibility classes. If the triggering threshold of a deposit exceeds the maximum anticipated ground motions for a low seismicity region, this deposit may be assigned a low susceptibility classification. However, if the triggering threshold of a deposit with similar geotechnical properties is exceeded in a more seismically active region, then this deposit should be assigned a higher

susceptibility rating. In preparing the combined liquefaction susceptibility map of the San Juan and Bayamon quadrangles we have evaluated the liquefaction triggering thresholds for each geological map unit and compared these triggering thresholds to three levels of ground shaking: 0.1g, 0.2g, and 0.3g. These are considered a reasonable range of ground motion accelerations that are likely to occur along the northern coast of Puerto Rico.

5.0 DEVELOPMENT OF COMBINED LIQUEFACTION SUSCEPTIBILITY MAPS

The liquefaction susceptibility mapping for the Bayamon Quadrangle followed the same methodology and approach as that used in mapping the San Juan Quadrangle (Hengesh and Bachhuber 1999, 2005) and is illustrated on Figures 4a and 4b. A common approach was used so that the two maps could be integrated into one combined map, while maintaining a level of consistency with the 1999 San Juan map. The liquefaction susceptibility mapping process involved five steps: (1) creating detailed Quaternary geologic maps delineating deposits of various age, depositional environment, and texture; (2) evaluating Quaternary deposit thickness and depth to groundwater; (3) performing initial evaluation of relative liquefaction susceptibility using a decision tree process; (4) evaluating liquefaction triggering thresholds using geotechnical borehole data and the Seed and Idriss (1971b) "Simplified Procedure"; and, (5) identifying units of similar susceptibility and grouping them to form liquefaction susceptibility zones.

The distribution of Quaternary map units was refined and augmented through original aerial photograph interpretation, field reconnaissance, and the evaluation of geotechnical borehole data. Because the lithologic and engineering properties of sediments often vary significantly both laterally and vertically, it is necessary to interpret the available surface and subsurface data to explain these variations and extrapolate borehole data to areas within similar map units that lack borehole data. The surficial geologic mapping provides the means to improve correlations among subsurface data and increase confidence in the distribution of susceptibility units.

6.0 LIQUEFACTION SUSCEPTIBILITY ANALYSIS

6.1 Quaternary Geologic Mapping

The Quaternary geologic map (Figure 3) was developed by compiling surficial geological and soils data, analyzing subsurface boring logs, interpreting aerial photographs, and conducting field verification of unit boundaries and descriptions. Data sources for our map analysis included:

- USGS geological map of the San Juan Quadrangle (scale 1:20,000) (Pease and Monroe, 1977);
- USGS geological map of the Bayamon Quadrangle (scale 1:20,000) (Monroe, 1973);
- Geology of the Middle Tertiary Formations of Puerto Rico (Monroe, 1980);
- Generalized Earthquake Induced Geologic Hazard Map for the San Juan Metropolitan Area at a scale of 1:40,000 (Molinelli-Freytes, 1985); and,
- Over 800 unpublished logs of geotechnical boreholes and water wells from the Puerto Rico Department of Transportation and Highways, Tren Urbano Project, local consultants, and U.S. Geological Survey files.

The published USGS quadrangle maps (Monroe, 1973; and Pease and Monroe, 1977) differentiate Quaternary deposits such as: stream channel, beach, swamp, dune, fluvial and marine terrace, alluvial fan, and artificial fill deposits. Approximate geological ages or relative ages are assigned to the units, and include information on general deposit thicknesses.

Quaternary map units for the Bayamon and San Juan quadrangles (Monroe, 1973 and Pease and Monroe, 1977) were reassessed to confirm unit boundaries, and textural characteristics, age and environment of deposition. Our re-evaluation consisted of (1) comparing geologic unit boundaries with stereographic interpretation of USGS (1937, 1962, 1997, and 2000) aerial photographs; (2) field reconnaissance of map units; and (3) analysis of borehole stratigraphy. Quaternary deposits and geomorphic surfaces were evaluated on the basis of several stratigraphic, geomorphic, and pedologic criteria, including: (1) topographic position in a sequence of inset deposits or surfaces; (2) relative degree of surface modification (e.g., erosional dissection); (3) relative degree of soil-profile development and other surface weathering phenomena; (4) superposition of deposits separated by erosional unconformities and/or buried soils; (5) relative ages of individual deposits; and (6) physical continuity and lateral correlation with other stratigraphic units. The resulting Quaternary geologic map used for our liquefaction susceptibility analysis is shown on Figure 2. Minor modifications to the map unit boundaries of Monroe (1973) and Pease and Monroe (1977) were made, including differentiation of older and younger alluvial deposits, differentiation of older and younger fan deposits, and adjustment of some contact locations. The geologic data were compiled at a scale of 1:20,000.

6.2 Evaluation of Quaternary Deposit Thickness and Depth to Groundwater

Subsurface data from 685 geotechnical borings and 130 water well logs were evaluated for both quadrangles to assess the texture and relative density of deposits, thickness of Holocene and Pleistocene sediments, and depth to groundwater. Data from the boring and well logs were used to define the unconformity that marks the Holocene-Pleistocene boundary and to estimate the thickness of potentially liquefiable Holocene sediments. In both the San Juan and Bayamon areas, the base of Holocene deposits is typically an irregular erosional surface recognized in geotechnical borings by a marked increase in SPT blow counts and in well logs by a lithologic change. Older deposits are generally finer grained than the overlying recent Holocene sediments, and represent a different paleo-landform or sedimentary environment than the modern setting. For example, coastal swamp deposits adjacent to Bahia de San Juan are within a modern broad topographic basin eroded into the distal parts of large coalescing alluvial fans and alluvial terraces. The swamp environment is conducive to deposition of loose, sandy and silty layers, and the composite thickness of the swamp deposits ranges between about 5 and 15 meters. A buried peat soil often marks the base of the Holocene deposits, but the thickness and depth to the peat layer varies from boring to boring. The underlying Pleistocene fan and alluvial deposits are more dense, and typically do not contain loose sediments susceptible to liquefaction.

Groundwater levels used in our liquefaction susceptibility analysis were assessed from geotechnical borings, well logs, and the topographic position of deposits relative to perennial streams and sea level. The depth to groundwater varied between map units, primarily due to differences in the elevations of landforms formed by the deposits and proximity to streams or water bodies. For example, Qs swamp deposits occur at or below mean sea level, older QTt alluvium lies in elevated terraces several meters above sea level. However, groundwater typically exists at depths less than about 3 to 7 meters across the entire study area, and is less than 1.5 meters deep under the coastal and lowland swamp areas. For the purposes of our liquefaction susceptibility analysis, we conservatively assumed that groundwater can rise to less than 1.5 meters across the entire study area.

6.3 Preliminary Liquefaction Susceptibility Evaluation with a Decision Tree

The liquefaction susceptibility of each map unit was initially estimated using the decision tree and data integration process illustrated on Figures 4a and 4b. The decision tree (Figure 4b) was developed specifically for the study area, and incorporates local geologic and groundwater occurrence factors that influence liquefaction susceptibility. This decision tree was modified from a similar one adopted by the California Geological Survey (Hitchcock et al., 1999). The results from the decision tree analyses were used to assign a susceptibility classification to each map unit that lacked sufficient subsurface data to quantitatively assess liquefaction triggering thresholds. The decision tree assigns the Very High susceptibility classification to late Holocene or modern deposits, and the High susceptibility classification to middle and early Holocene deposits. Older deposits are assigned to susceptibility classes that range from Very Low to Medium depending on the percent liquefiable texture, groundwater conditions, and SPT simplified procedure triggering levels. The percent liquefiable texture within a geologic unit was used to differentiate the susceptibility of more clay-rich deposits from deposits that lack clay and contain significant percentages of sand or silt. The percent liquefiable texture for each geologic unit was estimated on the basis of literature-reported characteristics (e.g. Monroe, 1973; Pease and Monroe, 1977), review of geotechnical boring and well logs, and field examination of deposits in stream banks and road cuts.

The decision tree also was used to define susceptibility classes where sufficient subsurface data were available to characterize liquefaction triggering threshold values. As described below, the liquefaction threshold analysis was based on the “Simplified Procedure” (Seed and Idriss, 1971b; Youd et al., 2001; 2003).

6.4 Evaluation of Borehole Data

Geotechnical borehole data were compiled to document subsurface stratigraphy, texture, soil density, and groundwater conditions for input to quantitative analysis of liquefaction susceptibility. A total of 685 geotechnical borings and 130 water well logs were evaluated for both quadrangles. In general, the geotechnical borings include detailed soil descriptions and information on soil density, whereas the well logs generally contain non-technical stratigraphic descriptions and are mainly useful to determine the depth to bedrock and major geologic stratigraphic units.

The geotechnical borings include SPT data for soils at various intervals throughout the boreholes, and also typically indicate depth to groundwater. The SPT is a standard method to evaluate the geotechnical properties of a soil deposit. The SPT data are obtained by driving a hollow sampler of standardized dimensions into the bottom of a borehole with standardized hammering equipment, and recording the hammer blows (“N” count) required to drive the sampler in 6-inch increments for a total drive length of 18-inches. The resulting SPT “N” count is recorded by totaling the blows required to drive the sampler the last 12-inches of penetration. The SPT tests in the area were obtained by local drilling companies using standardized 140-pound hammers with 30-inch drop heights. Typically, cathead or wireline hammer triggering equipment was used.

The "Simplified Procedure" was used to assess quantitatively the susceptibility of a deposit to liquefaction given various levels of ground shaking (Seed and Idriss, 1971b; Seed et al., 1983; Seed and Harder, 1990). The Simplified Procedure is an empirically-based method used to compute the peak ground acceleration (PGA) liquefaction triggering threshold that considers the percent fines content, groundwater conditions, overburden loads, SPT-based density correlations, and earthquake loading conditions (cyclic stress ratio, or CSR) for silty and sandy sediments. The Simplified Procedure allows estimation of the ground motion triggering threshold that could initiate liquefaction in susceptible deposits. We note that the San Juan liquefaction susceptibility study was performed between 1996 and 1998, and incorporated the various Simplified Procedure correlations and methodologies that were standard practice at this time. The Simplified procedure has since been modified (e.g., Youd et al., 2001; 2003), but the more recent modifications do not affect the relative liquefaction susceptibility classifications established for our study.
The liquefaction triggering thresholds were estimated for three scenario earthquakes that are considered likely in the region. These included Mw 8.0 and Mw7.5 events located along the Puerto Rico subduction zone, and a Mw 6.5 event located onshore in proximity to San Juan. In the analyses we also specified three levels of PGA that might be produced from these scenario earthquakes. The ground motions considered are 0.1g, 0.2g, and 0.3g. These ground motion values were based on the tectonic environment of the San Juan region, as well as previous ground motion assessments for the area (i.e. Mueller et al, 2003 and Crouse and Hengesh, 2003), and are considered realistic values with a moderate to high probability of occurrence. In addition to evaluation of different PGA levels, the effects of different strong ground shaking durations from the range of scenario earthquake magnitudes were analyzed using magnitude correction factors (Seed et al., 1983; Seed and Harder, 1990). For equivalent PGA levels, the increased duration from larger magnitude earthquakes causes increased occurrence of liquefaction.

The liquefaction susceptibility analysis for each map unit from the San Juan Quadrangle was performed by calculating whether or not a deposit from the uppermost 20 meters of sediment would liquefy for the three scenario ground motions produced from the three distinct scenario earthquakes. We compiled geotechnical data for each geologic map unit into separate Excel worksheets, and performed the Simplified Procedure analyses in conjunction with the decision tree evaluation (Figure 4b). This allowed comparison of the liquefaction susceptibility and PGA triggering threshold of distinct map units to establish the relative susceptibility ranking (Figure 4a).

Figure 5 shows summary liquefaction susceptibility plots from the Simplified Procedure analysis for six San Juan Quadrangle map units based on the Mw7.5 scenario earthquake. The plotted SPT data are for deposits described as "silt" or "sand" on the geotechnical boring for the Qs Holocene swamp, Qb Holocene beach, Qay Holocene alluvium, Qss early Holocene-late Pleistocene silica sand, Qf Pleistocene alluvial fan and valley fill, and QTt Pleistocene-Pliocene alluvium. The summary plots show the amount and variability of SPT data from each map unit. The SPT data are plotted in three populations that represent the 0.1g, 0.2g, and 0.3g input ground motions. The plots also show three curves ("boundary curves") that are used to evaluate whether a sample would liquefy or not based on the percent clay fraction of the soil. Points that plot to the left of a boundary curve have exceeded the liquefaction triggering threshold and are potentially liquefiable, and points to the right are below the liquefaction triggering threshold and are not expected to liquefy.

The three populations represented on the plots (e.g. 0.1g, 0.2g, and 0.3g) allow a quantitative evaluation of the ground shaking triggering level. By visually inspecting the mean value of each SPT blow count cluster, we determine at what PGA level the mean value falls to the left of the boundary curve. This PGA value is then selected as the general PGA triggering level for that map unit. Additionally, visual comparison of the Figure 5 plots allows evaluation of the relative liquefaction susceptibility of the various map units. For example, the plot for young alluvium (Qay) on Figure 5 indicates that for 0.1g the majority of the data points fall to the right of the liquefaction boundary curves and therefore would not trigger into liquefaction at this ground motion level. However, for ground motions of 0.2g or greater, most data points fall to the left of the boundary curves, and therefore would be triggered into liquefaction. The estimated triggering PGA values for each map unit (Table 1) were used to augment the liquefaction susceptibility classifications (e.g. high, medium and low) presented on the decision tree (Figure 4b). The subsurface data for the Bayamon Quadrangle also were assessed and considered to be similar to those from the San Juan quadrangle. Therefore, the relative susceptibility classifications were similarly defined. The resulting combined liquefaction susceptibility map is shown on Figure 6.

7.0 RESULTS - LIQUEFACTION SUSCEPTIBILITY MAP

The Liquefaction Susceptibility Map shown on Figure 6 illustrates the general susceptibility of the San Juan and Bayamon areas to liquefaction. This map was prepared by integrating the various map and data layers and the susceptibility ranking decision tree shown on Figure 4b, and the Simplified Procedure analyses described above and shown on Figure 5. The susceptibility analysis considered Mw 6.5, Mw 7.5 and Mw 8.0 scenario earthquakes, and estimated PGA values of 0.1g, 0.2g, and 0.3g. The analysis shows that that the triggering threshold values for Mw 6.5 and Mw 8.0 scenario earthquakes bracket the range of values and thus were used in establishing the relative susceptibility rankings (Table 1). Seven relative susceptibility zones were established: Very High, High, Medium to High, Medium, Low to Medium, Low, and Very Low. Each of these zones has different estimated PGA liquefaction triggering levels (Table 1; Figures. 4b, 5 and 6).

In general, zones ranked as Very High and High susceptibility could potentially experience widespread and severe liquefaction under moderate to strong earthquake shaking, and possible minor to moderate liquefaction under moderate levels of earthquake shaking. Zones ranked as Low and Very Low susceptibility likely would either experience no significant liquefaction, or isolated and relatively minor liquefaction even under very strong earthquake shaking. The Medium susceptibility zones likely would experience isolated and restricted zones of severe to moderate liquefaction under strong earthquake shaking, and only very minor and sparse liquefaction under moderate levels of earthquake shaking.

7.1 Very High Susceptibility Zones

The Very High susceptibility zones (Figure 6) comprise modern swamp deposits (Qs) and areas of artificial fill over swamp deposits (Qaf/Qs) in the reclaimed areas along the Bayamon coastal plain and around Bahia de San Juan and Laguna San Jose (Figure 3). Silt and sand lenses in these deposits have estimated PGA liquefaction triggering thresholds of 0.05 to 0.1 g, and have estimated liquefiable texture of about 50 percent. Groundwater in these deposits is generally encountered within about 1.5 meters of the ground surface. These deposits occur in lagoons, swamps and estuaries (collectively referred to as swamps) or under filled land along swamp margins, and generally consist of soft, unconsolidated, saturated sediment including silt, clay, peat, and discontinuous sand lenses. Borings show that the silt and sand composition of these deposits is higher near the mouths of streams that discharge into swamps, and where sand is blown inland from beaches and sand spits along swamp margins. However, silt and sand lenses can occur throughout the swamp deposits. Artificial fill overlying swamp deposits (Qaf/Qs,) is commonly saturated, and varies locally in composition and density. The liquefaction susceptibility of artificial fill ranges from Low (coarse rocky clay fill) to Very High (fine sand and silt hydraulic fill), and conservatively should be considered to be Very High where fill overlies swamp deposits until proven otherwise by site-specific studies. Liquefaction of silt and sand lenses in swamp deposits underlying fill also can cause differential settlement, lateral spreading, oscillation, and fissuring of non-liquefied overlying fill.

Although the Qs and Qaf/Qs deposits have the highest susceptibility to liquefaction in the region, the surface manifestations of liquefaction may vary due to the presence of lenticular sand bodies, areas of clayey or fine silt, and/or peat deposits. Surface expression of liquefaction is likely to vary considerably within these units; we conservatively estimate that liquefaction in the most susceptible Qs and Qaf/Qs units may be expressed over 25% to 50% of the surface area. Liquefaction occurrence and effects likely will be concentrated and of greatest magnitude within 100 meters of the coastal margin, and 50 meters of stream channels or free faces.

7.2 High and Medium to High Susceptibility Zones

The High susceptibility zone consists of late Holocene alluvial channels (Qac) and Holocene beach deposits (Qb), which are comprised primarily of sand and silty sand (estimated sand and silt percentages of less than 80 percent), and occur in low areas with a relatively high groundwater table generally less than about 1.5 meters deep. The Qac unit is assigned a High liquefaction susceptibility rating with a PGA triggering threshold of 0.1 to 0.15g and Qb units are assigned a Medium to High liquefaction susceptibility rating with a PGA triggering threshold of 0.1 to 0.2 g. We conservatively estimate that liquefaction may occur over 25% of this map unit.

7.3 Medium Susceptibility Zone

The Medium susceptibility zone consists of five map units: late Pleistocene to Holocene Terraces (Qt); artificial fill (Qaf); artificial road embankment fill (Qafe); Holocene alluvium (Qay) such as channel sediments or low floodplain and terrace deposits along active streams; and artificial fill over alluvium (Qaf/Qay). These units typically consists of interbedded clay, silt, and sand with some gravel lenses and have estimated PGA triggering threshold of 0.15 to 0.25g. The liquefiable texture ranges between about 35 and 50 percent, and groundwater levels range from about 1.5 to 6 meters deep. Portions of the beach deposits (Qb) also fall within the Medium-susceptibility zone, although these have been conservatively assigned to the High-susceptibility zone, as described above.

We estimate that liquefaction in the Medium susceptibility zones will be localized, probably not exceeding 10% of the mapped unit, and be concentrated adjacent to stream channels.

7.4 Low to Medium and Low Susceptibility Zones

The Low and Low to Medium susceptibility zones consist of six main map units: the Santurce Sands or Silica Sands (Qss), which are stabilized and generally cemented Pleistocene dune deposits; valley fill (Qvf) which represents the well graded clayey gravel sediment accumulations in small tributary drainages; Pleistocene-aged alluvium and alluvial fan deposits (Qf, Qfo, Qao), and early Pleistocene “blanket deposits” (QTb) that include colluvium and regolith (primarily in the Bayamon Quadrangle). Analysis of borehole data suggests that groundwater levels are about 1.5 to 10 meters depth, and where suitable liquefiable texture is present in these deposits the PGA liquefaction triggering thresholds are greater than 0.25 to 0.3g. These deposits generally contain liquefiable textures of about 10 to 30 percent. The Santurce Sands (Qss) unit contains about 80 percent liquefiable texture, but exhibits a high degree of packing, and possible weak ferruginous or silica cementation that should preclude development of extensive liquefaction. If liquefaction occurs in the Low susceptibility zone, it would likely be of very limited areal extent (less than about 5% of map area). We would not expect significant settlement or lateral spreads in this unit.

7.5 Very Low Susceptibility Zone

The Very Low susceptibility zone is comprised of late Tertiary to early Pleistocene alluvium (QTt) that occurs in fans and terraces along the southern edge of the San Juan basin, and along Rio Bayamon and Rio de la Plata. These materials exhibit dense grain packing and incipient stages of lithification. Groundwater typically is between 3 and 10 meters deep. Analysis of borehole data indicates a PGA liquefaction triggering threshold of over 0.3g for unlithified sandy sediments within these deposits, however we believe that aging effects and overconsolidation of these deposits would prevent development of liquefaction.

Bedrock units are considered to have a negligible liquefaction hazard.

8.0 DISCUSSION

The combined liquefaction susceptibility map is shown on Figure 6. The unit-specific PGA triggering thresholds can be used to estimate which map areas could undergo liquefaction during future earthquakes by comparing ground motion levels to the estimated liquefaction triggering thresholds. Liquefaction occurrence is not expected to be uniform within the susceptibility zones, and liquefaction would be concentrated and most severe where ground motions significantly exceed the triggering values, rather than in zones where the ground motion levels are the same as, or slightly greater than, the triggering values. For the purposes of general planning, the areas of most severe liquefaction related ground deformation are likely to occur within the swamp and artificial fill over swamp deposits, and within roughly 100 meters of shorelines, stream channels, and drainage channels (free face zones).

Most liquefaction-induced damage is caused by differential ground settlement, surface cracking, loss of bearing capacity, and lateral spread movements (Seed and Idriss, 1971a). The occurrence of liquefaction does not always cause these effects, particularly if the liquefaction occurs on level ground and/or the liquefied layer is deeply buried. For example, although liquefaction occurred over approximately 10,000 km2 during the January 2001 Mw 7.7 Bhuj, India earthquake, lateral spread failures were restricted to only a few locations associated with dipping subsurface units or free-faces (Hengesh and Lettis, 2002; Tuttle et al., 2002). Additionally, liquefaction-induced ground failure during the 1999 Kocaeli earthquake in Turkey and 1995 Kobe earthquake in Japan typically were restricted to areas where liquefied layers are thick and occur at shallow depth, and within about 100 meters of shorelines and free faces such as stream banks and coastlines (e.g., Hamada et. al, 1995; Rathje and others, 2003). Microzonation of these areas and quantification of liquefaction-induced effects requires dense borehole data and specific engineering analyses that are beyond the scope of this regional susceptibility mapping study. However, general estimates of potential settlement and lateral spread movement can be made for the various susceptibility map zones using the PGA triggering threshold values, estimated thickness of deposits, and percentage of liquefiable texture listed in Table 1. Quantitative estimates of the potential settlements and lateral spreads can be developed with empirically based methods developed by Ishihara and Yoshimine (1992) to predict magnitude of settlement, and by Bartlett and Youd (1995) to predict amount of lateral spread movement.

9.0 CONCLUSIONS

A combined liquefaction susceptibility map was prepared for the Bayamon and San Juan quadrangles, Puerto Rico. This map was developed through integration of Quaternary geological data with subsurface data from geotechnical borings and well logs. The hazard characteristics of each significant map unit were established so that geological map units of similar hazard rating could be combined to form relative liquefaction susceptibility hazard zones.

The resulting liquefaction susceptibility map (Figure 6) shows the relative hazard across the greater San Juan metropolitan area. The liquefaction susceptibility map shows that the areas of Very High hazard occur within the northern parts of the San Juan and Bayamon quadrangles, specifically along the Bayamon coastal plain, and the edges of Bahia de San Juan and Laguna San Jose. Extensive swamp deposits and artificial fill over swamp deposits occur in these areas. These deposits contain layers of young, saturated, and cohesionless silt and sand. The High liquefaction hazard zone includes the abandoned river and stream channels common near Rio Bayamon and Rio de la Plata, and along the beach and areas in the vicinity of the airport. Damage to structures or lifeline facilities from liquefaction in these areas may be extensive during future earthquakes if appropriate design or mitigation measures are not properly implemented. Most of the area to the south of Sabana Seca, Bahia de San Juan and Laguna San Jose lie within Medium, Low, or Very Low hazard zones.

Special consideration of the effects of liquefaction should be given during the site selection, design and construction of structures and underground improvements, especially in the High and Very High hazard zones. The presence of these zones should not prohibit development, but rather should be used as an initial indication that subsurface conditions may warrant site-specific investigations and/or engineering solutions to mitigate the potential affects of liquefaction. Development within these types of hazard zones is becoming routine engineering practice and the hazards associated with liquefaction can generally be mitigated or avoided.

10.0 ACKNOWLEDGEMENTS

This research was supported by the U.S. Geological Survey, Department of the Interior, under USGS award number 03HQGR0107. The views and conclusions in this document are those of the authors and should not be interpreted as necessarily representing the official policies, either expressed or implied, of the U.S. Government. Numerous people and agencies helped with data compilation for the study, including Mr. Richard Webb of the Bayamon Office U.S. Geological Survey, Dr. Juan Carlos Moya, Director Ariel Perez and (past Director) Jose Hernandez of the Autoridad de Carreteras y Transportacion, Mr. Mariano Vargas of the Civil Defense, and the late Dr. Jose Capacetti. Special thanks and gratitude are extended to Derrick Stepanof and Alex Soto, local consulting geologists who provided valuable insight and subsurface information. Data integration into the Puerto Rican Office of Governor Planning Board GIS database was facilitated by Analyst Rebecca de la Cruz Perez.

11.0 REFERENCES

Bachhuber, J.L., Thompson, S.C., Noller, J.S., and Lettis, W.L., 1994, Liquefaction susceptibility mapping of the San Francisco Bay Area, California [abs.]: Geological Society of America Annual Meeting, October, 1994, Seattle, Washington.

Bartlett, S.F., and Youd, T.L., 1995, Empirical prediction of liquefaction-induced lateral spreads: Journal Geotechnical engineering: American Soc. of Civil Engineers, v. 121, no. 4, p. 316-329.

Birkeland, P.W., 1984, Soils and Geomorphology, Oxford University Press, p. 372.

Crouse, C.B., and Hengesh, J.V., 2003, Probabilistic seismic hazard analysis for Puerto Rico, Seismological Society of America, 73rd Annual Meeting Program with Abstracts, Seismological Research Letters, v. 74, no. 2, p. 206.

Dolan, J. F., and Wald, D. J., 1998, The 1943 – 1953 north-central Caribbean earthquakes: Active tectonic setting, seismic hazards and implications for Caribbean-North America plate motions, in Active Strike-Slip and Collisional Tectonics of the Northern Caribbean Plate Boundary Zone, edited by J. F. Dolan and P. Mann, Geological Society of America Special Paper, 326, 143 – 169.

Doser, D.I., Rodriguez, C.M., and Flores, C., 2005, Historical earthquakes of the Puerto Rico-Virgin Islands region (1915-1963), in Mann, P., ed., Active tectonics and Seismic Hazards of Puerto Rico, the Virgin Islands, and offshore areas: Geological Society of America Special Paper, 385, p. 249-262.

Ellis, S.R., 1976, History of dredging and filling of lagoons in the San Juan area, Puerto Rico: U.S. Geological Survey Water Resources Investigations No. 38-76, 25 p.

Hamada, M., Isoyama, R. and Wakamatsu, K., 1995, The 1995 Hyogoken-Nanbu (Kobe) earthquake, liquefaction, ground displacement and soil condition in Hanshin area: Association for Development of Earthquake Prediction, Waseda University and Japan Engineering Consultants, p. 194.

Hengesh, J.V. and Bachhuber, J.L., 2005, Liquefaction susceptibility zonation map of San Juan Puerto Rico, in Mann, P., ed., Active tectonics and Seismic Hazards of Puerto Rico, the Virgin Islands, and offshore areas: Geological Society of America Special Paper, 385, p. 249-262.

Hengesh, J.V., and Lettis, W.R., 2002, Tectonic setting and geological effects of the Mw 7.7 2001 Bhuj Earthquake: EERI Special Publication on the Bhuj earthquake.

Hengesh, J.V., and Bachhuber, J.L., 1999, Seismic Zonation of the Greater San Juan Metropolitan Area, Puerto Rico: Final Technical Report, U.S. Geological Survey National Earthquake Hazard Reduction Program.

Hitchcock, C.S., Lloyd, R.C., and Haydon, W.D., 1999, Mapping liquefaction hazards in Simi Valley, Ventura County, California: Association of Engineering Geologists Environmental and Engineering Geosciences, v. 5, no. 4, p. 441-458.

Horsfield, W.T., 1975, Quaternary Vertical Movements in the Greater Antilles: Geological Society of America Bulletin, v. 86, p. 933-938.

Ishihara, K. and Yoshimine, M., 1992, Evaluation of settlements in sand deposits following liquefaction during earthquakes: Soils and Foundations, v. 32, no.1, March, p. 173-188.

Mann, P. Hippolyte, J.C., Grindlay, N.R., and L.J. Abrams, 2005, Neotectonics of southern Puerto Rico and its offshore: Geological Society of America, Special Paper 385, p. 173.

Mann, P., Calais, E., Ruegg, J.C., DeMets, C., Jansma, P.E., and Mattioli, G.S., 2002, Oblique collision in the northeastern Caribbean from GPS measurements and geological observations: Tectonics, vol. 21, no. 6, p. 1057.

Masson, D.G., and Scanlon, K.M., 1991. The neotectonic setting of Puerto Rico: Geological Society of America Bulletin, v. 103, pp. 144-154.

McCann, W.R., 2002, Microearthquake data elucidate details of the Caribbean subduction zone: Seismological Research Letters v. 73, no. 1, p. 25-32.

McCann, W.R., and Pennington, W.D., 1990, Seismicity, large earthquakes, and the margin of the Caribbean plate, in The Geology of North America, The Caribbean Region, Vol. H, edited by Dengo, G., and Case, J.E., Geol. Soc. of Amer., p. 291.

Mitchell, J.K., 1999, Fundamentals of soil behavior: John Wiley & Sons, Inc., New York, p. 437.

Monroe, W.H., 1968, High-level Quaternary beach deposits in northwestern Puerto Rico: U.S. Geological Survey Professional Paper 600-C, p. C140-143.

Monroe, W.H., 1973, Geologic Map of the Bayamon Quadrangle, Puerto Rico: U.S. Geological Survey Miscellaneous Geologic Investigations Map I-751, scale 1:20,000.

Monroe, W.H., 1980. Geology of the middle Tertiary formations of Puerto Rico: U.S. Geological Survey Professional Paper 953.

Molinelli-Freytes, J.M., 1985, Generalized earthquake induced geologic hazards map for the San Juan Metropolitan area, Commonwealth of Puerto Rico, Department of Natural Resources, Planning Resources Area, unpublished map, scale 1:40,000.

Mueller, C.S., Frankel, A.D., Petersen, M.D. and Leyendecker, E.V., 2003, Documentation for 2003 USGS Seismic Hazard Maps for Puerto Rico and the U.S. Virgin Islands, http://geohazards.cr.usgs.gov/eq/html/prvi2003.html

Pease, M.H. Jr., and Monroe, W.H., 1977, Geologic map of the San Juan Quadrangle, Puerto Rico: U.S. Geological Survey Miscellaneous Geologic Investigations Map I-1010, scale 1:20,000.

Pyke, R., 2003, Discussion of "Liquefaction Resistance of Soils: Summary Report from the 1996 NCEER and 1998 NCEER/NSF Workshops on Evaluation of Liquefaction Resistance of Soils " by Youd, T.L., Idriss, I.M. Andrus, R.D. Arango, I., Castro, G., Christian, J.T., Dobry, R., Liam Finn, W.D.L., Harder, L.F., Jr., Hynes, M.E., Ishihara, K., Koester, J.P., Liao, S.S.C., Marcuson, W.F., III, Martin, G.R., Mitchell, J.K., Moriwaki, Y., Power, M.S., Robertson, P.K., Seed, R.B., Stokoe, K.H., II": ASCE: Journal of Geotechnical and Geoenvironmental Engineering, v. 129, No. 3, p. 283-284.

Rathje, E.M., Karatas, I., and Bachhuber, J., 2003, Evaluation of integrated seismic hazards and ground failure in pull-apart basins during the 1999 Kocaeli earthquake, Turkey: U.S. Geological Survey Technical Report, NEHRP Research Award 02HQGR0030.

Reid, H. and Taber, S., 1919, The Porto Rico earthquake of 1918, with descriptions of earlier earthquakes. Report of the Earthquake Investigation Commission, House of Rep. Doc. 269, Washington, D.C., p. 74.

Seed, R.B., and Harder, L.F., 1990, SPT-based analysis of cyclic pore pressure generation and undrained residual strength, *in* Duncan, M.J., editor, H. Bolton Seed Memorial Symposium Proceedings, May, 1990: BiTech Publishers, Vancouver, B.C., Canada, p. 351-376.

Seed, H.B., and Idriss, I.M., 1971a, Influence of soil conditions on building damage potential during earthquakes. Journal of the Structural Division, American Society of Civil Engineers, Vol. 97, No. ST2, Proceedings Paper 7909, pp. 639-663.

Seed, H.B., and Idriss, I.M., 1971b, Simplified procedure for evaluating soil liquefaction potential. Proceeding of the American Society of Civil Engineers, Journal of the Soil Mechanics and Foundations Division, v. 93, no. SM9, pp. 1249-1273.

Seed, H.B., Idriss, I.M., and Arango, I., 1983, Evaluation of liquefaction potential using field performance data. American Society of Civil Engineers, Journal of Geotechnical Engineering, v. 109, no. 3, p. 458-482.

Seed, R.B., Cetin, K.O., Moss, R.E.S., Kammerer, A.M., Wu., J., Pestana, J.M., and Riemer, M.F., 2002, Recent advances in soil liquefaction engineering and seismic site response evaluation, Paper No. SPL-2.

Taggert, B.E., and Joyce, J., 1989, Radiometrically dated marine terraces on northwestern Puerto Rico: in Larue, D.K. and Draper, G., eds., Transactions of the 12th Caribbean Conference, St. Croix, U.S. Virgin Islands; Miami Geological Society, Coral Gables, Florida, p. 248-256.

Tinsley, J.C., Youd, T.L., Perkins, D.M., and Chen, A.T.F, 1985. Evaluating liquefaction potential, in Ziony, J.I., ed., Evaluating earthquake hazards in the Los Angeles Region -an earth-science perspective: United States Geological Survey Professional Paper 1360, pp. 263-316.

Tuttle, M.P., Hengesh, J.V., Lettis, W.R., and Tucker, K., 2002, Observations and comparisons of liquefaction features and related effects induced by the Bhuj earthquake: EERI Special Publication on the Bhuj earthquake.

Tuttle, M. P., Dyer-Williams, K., Schweig, E.S., Prentice, C.S., Moya, J.S., and Tucker, K.B., 2005, Liquefaction induced by historic and prehistoric earthquakes in western Puerto Rico: in Mann, P., ed., Active tectonics and Seismic Hazards of Puerto Rico, the Virgin Islands, and offshore areas: Geological Society of America Special Paper, 385, p. 249-262.

U.S. Geological Survey, February 16, 1962. Aerial Photographs: GS-VAIH XF-6745 5-92 to 5-101; 5-120 to 5-130; 5-80 to 5-89; and 5-6 to 5-9.

Youd, T.L.; and Perkins, D.M., 1978, Mapping liquefaction-induced ground failure potential: Journal of Geotechnical Engineering, v. 104 no.4, p. 433-446.

Youd, T.L., 1991, Mapping of earthquake-induced liquefaction for seismic zonation, in Proceedings Fourth International Conference on Seismic Zonation: Earthquake Engineering Research Institute, August 1991, Stanford University, p.111-138.

Youd, T.L., Idriss, I.M. Andrus, R.D. Arango, I., Castro, G., Christian, J.T., Dobry, R., Liam Finn, W.D.L., Harder, L.F., Jr., Hynes, M.E., Ishihara, K., Koester, J.P., Liao, S.S.C., Marcuson, W.F., III, Martin, G.R., Mitchell, J.K., Moriwaki, Y., Power, M.S., Robertson, P.K., Seed, R.B., Stokoe, K.H., II, 2001, Liquefaction Resistance of Soils: Summary Report from the 1996 NCEER and 1998 NCEER/NSF Workshops on Evaluation of Liquefaction Resistance of Soils, ASCE: Journal of Geotechnical and Geoenvironmental Engineering, v. 127, no. 10, p. 817-833.

Youd, T.L., Idriss, I.M. Andrus, R.D. Arango, I., Castro, G., Christian, J.T., Dobry, R., Liam Finn, W.D.L., Harder, L.F., Jr., Hynes, M.E., Ishihara, K., Koester, J.P., Liao, S.S.C., Marcuson, W.F., III, Martin, G.R., Mitchell, J.K., Moriwaki, Y., Power, M.S., Robertson, P.K., Seed, R.B., Stokoe, K.H., II, 2003, Closure to “Liquefaction Resistance of Soils: Summary Report from the 1996 NCEER and 1998 NCEER/NSF Workshops on Evaluation of Liquefaction Resistance of Soils”, ASCE: Journal of Geotechnical and Geoenvironmental Engineering, v. 129, no. 3, p. 284-286.

Table 1. Liquefaction Susceptibility Values

Geologic Unit	Description	Estimated Percent Liquefiable Texture	Estimated Liquefaction Triggering Acc.		Typical Groundwater Depth (m)	Liquefaction Hazard *
			M_w 6.5	M_w 8.0		
Qs	Holocene swamp deposits	50%	0.1g	0.05g	<1.5'	**VERY HIGH**
Qaf/Qs **	Artificial fill over swamps	<50%	0.1-0.2g	0.05-0.15g	<3.0'	**VERY HIGH (See Note 2)**
Qac	Late Holocene alluvial channels	<75%	0.15g	0.1g	<1.5'	**High**
Qb	Holocene beach deposits	80%	0.15-0.2g	0.1-0.15g	<1.5'	**MEDIUM-HIGH**
Qt	Late Pleistocene to Holocene terrace	35%	0.2g	0.15g	<3.0'	**MEDIUM**
Qaf	Artificial fill	<50%	0.2g	0.15g	1.5-6.0	**MEDIUM**
Qafe	Artificial road enbankment fill	<50%	0.25g	0.15-0.2g	1.5-6.0	**MEDIUM**
Qay	Holocene alluvium	40%	0.2g	0.15g	<3.0'	**MEDIUM**
Qaf/Qay	Artificial fill over alluvium	<50%	0.2g	0.15g	1.5-6.0	**MEDIUM**
Qss	Late Pleistocene(?) dune sands	80%	>0.3g	>0.2g	3.0-10	**LOW-MEDIUM**
Qvf	Late Pleistocene to Holocene valley fill	<30%	>0.3g	>0.25g	1.5-6.0	**LOW**
Qf	Late Pleistocene to early Holocene fan	<10%	>0.3g	>0.25g	1.5-6.0	**LOW**
Qfo	Mid Pleistocene to Pliocene fan deposits	<10%	>0.3g	>0.3g	1.5-6.0	**LOW**
Qao	Late Pleistocene-Pliocene alluvium	<30%	>0.3g	>0.25g	1.5-6.0	**LOW**
Qtb	Late Pleistocene to Holocene blanket	<10%	>0.3g	>0.25g	1.5-6.0	**LOW**
QTt	Pleistocene alluvium	<10%	>0.3g	>0.3g	3.0-10	**LOW-VERY LOW**
Bx	Bedrock	0%	NA	NA	3.0-10	**NEGLIGIBLE**

* Triggering accelerations shown are for Peak Ground Acceleration (PGA). Estimated triggering levels are based on evaluation of borehole Standard Penetration Test data using Seed and Simplified Approach (Seed et al., 1971). The triggering values should be viewed as approximations, and should be verified by site specific studies.

** Susceptibility is dependent on density of fill, which is quite variable. For initial screening, area should be considered to have high susceptibility until proven otherwise by additional information.

FIGURES

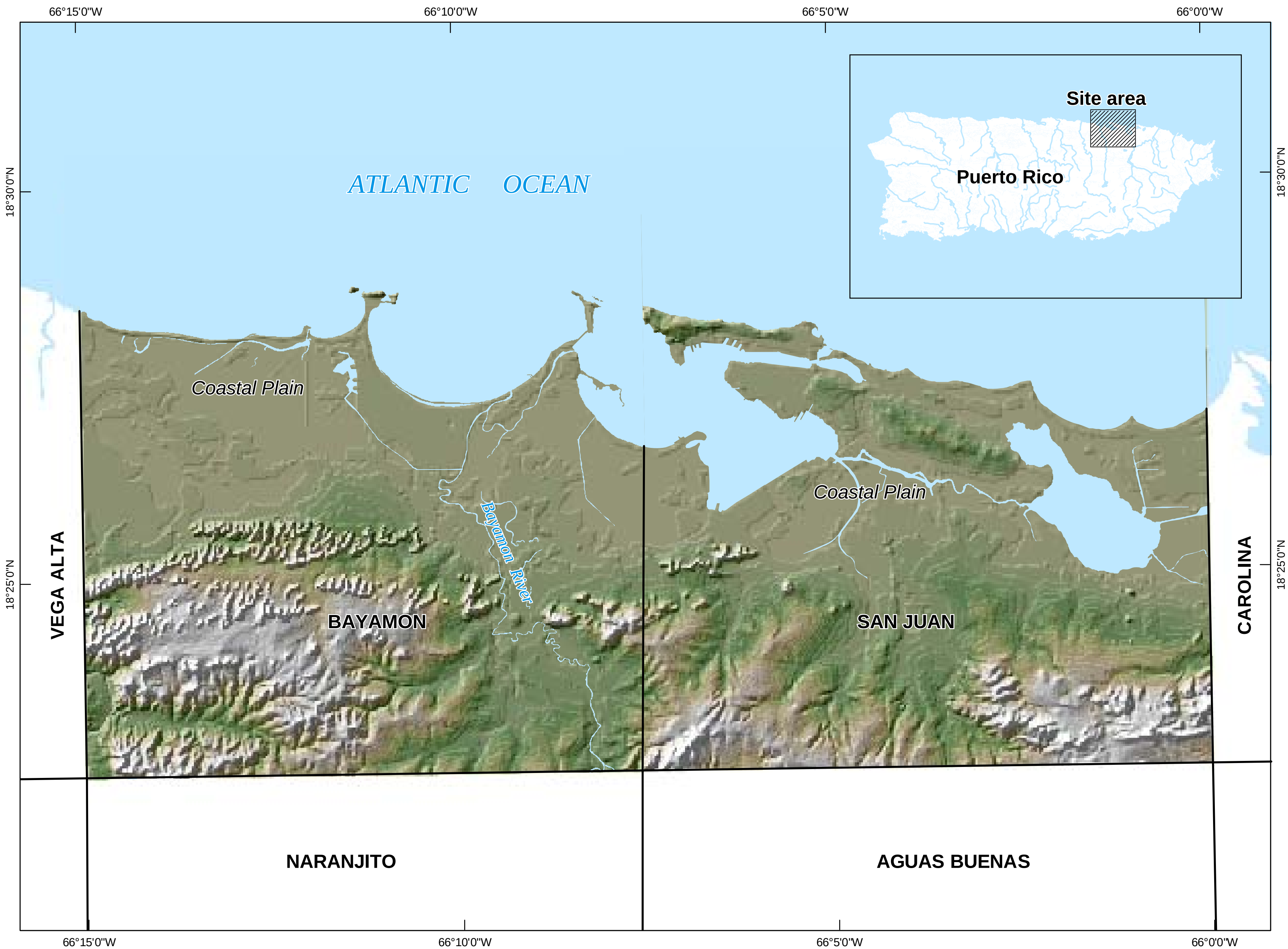

Figure 1. U.S.G.D. topographic quadrangle sheets and topographic relief map showing study area.

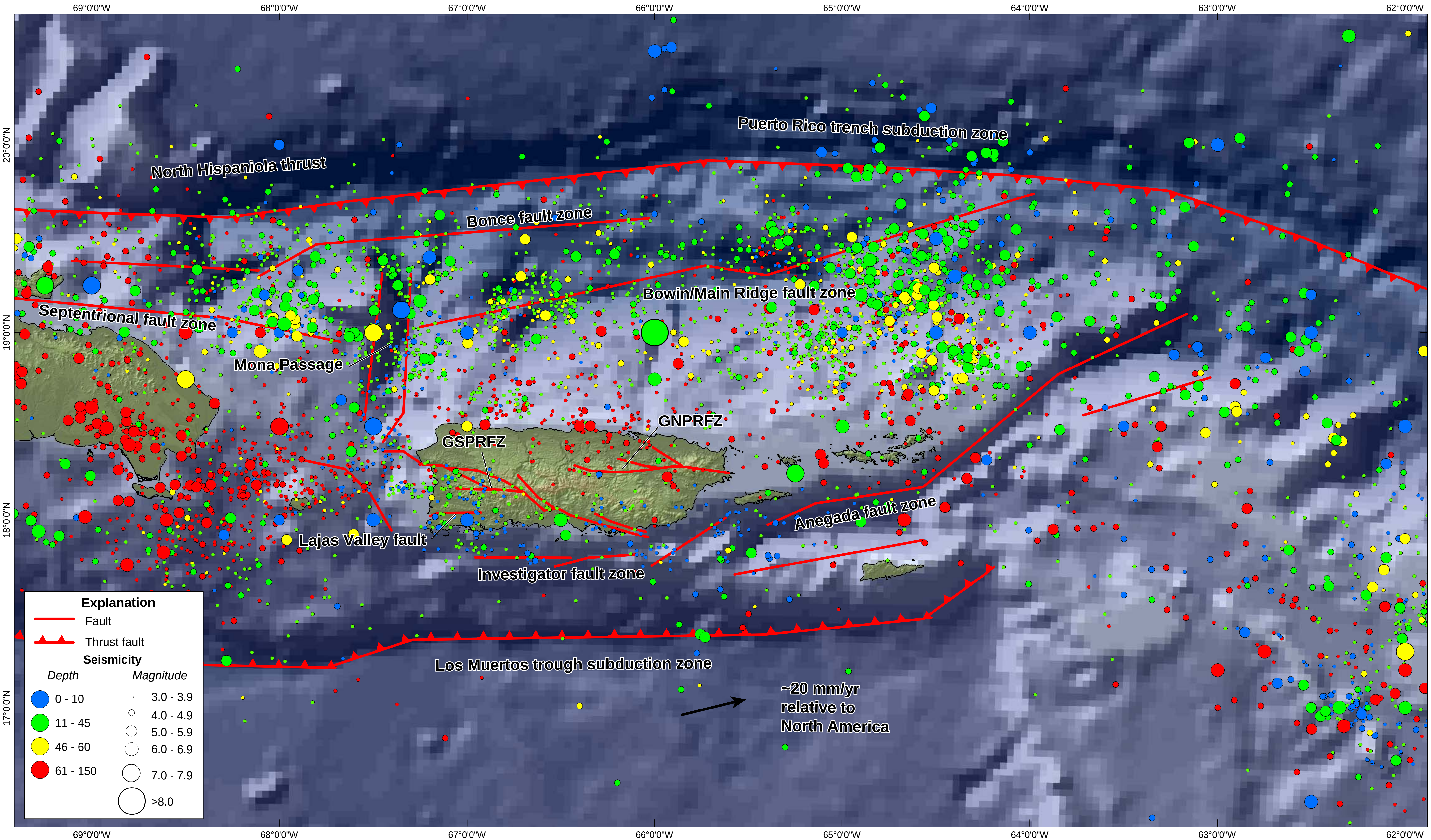

Notes: 1. From Dolan and Wald, 1998.
2. GNPRFZ = Great Northern Puerto Rico fault zone;
GSPRFZ = Great Southern Puerto Rico fault zone.

Figure 2. Regional tectonic setting.


Explanation
Bayamon Geology
USGS well
Geotech boring
San Juan Geology
San Juan boring
Unit Descriptions
Bx Bedrock
Qac Late Holocene alluvial channel
Qaf Artificial fill
Qaf/Qay Artificial fill over alluvium
Qaf/Qs Artificial fill over swamps
Qao Late Pleistocene-Pliocene alluvium
Qay Holocene alluvium
Qb Holocene beach deposits
Qbr Holocene beach rock
Qf Late Pleistocene to early Holocene fan deposits
Qf/Qs Artificial fill over swamp
Qs Holocene swamp deposits
Qss Late Pleistocene(?) dune sands
Qt Late Pleistocene to Holocene terrace deposits
Qtb Late Pleistocene to Holocene blanket deposits
Qvf Late Pleistocene to Holocene valley fill
Water
Unit Descriptions
Bx Bedrock
Qaf Artificial fill
Qaf/Qs Artificial fill over alluvium
Qafe Artificial road enbankment fill
Qao Late Pleistocene-Pliocene alluvium
Qay Holocene alluvium
Qb Holocene beach deposits
Qf Late Pleistocene to early Holocene fan deposits
Qfo Mid Pleistocene to Pliocene fan deposits
Qs Holocene swamp deposits
Qss Late Pleistocene(?) dune sands
Qtb Late Pleistocene to Holocene blanket deposits
Qvf Late Pleistocene to Holocene valley fill
Water
Water
N
0 2600 5200 feet
ATLANTIC OCEAN
SAN JUAN
BAHIA DE SAN JUAN
UNITED STATES
DEPARTMENT OF THE INTERIOR
GEOLOGICAL SURVEY
COMMONWEALTH OF PUERTO RICO
DEPARTMENT OF TRANSPORTATION AND PUBLIC WORKS
BAYAMON QUADRANGLE
PUERTO RICO
7.5 MINUTE SERIES (TOPOGRAPHIC)
LIQUEFACTION SUSCEPTIBILITY OF THE BAYAMON AND SAN JUAN QUADRANGLES, PUERTO RICO
Surficial Geology Map
WLA WILLIAM LETTIS & ASSOCIATES, INC.
Figure 3
01.23.08
1580 Bayamon NEHRP

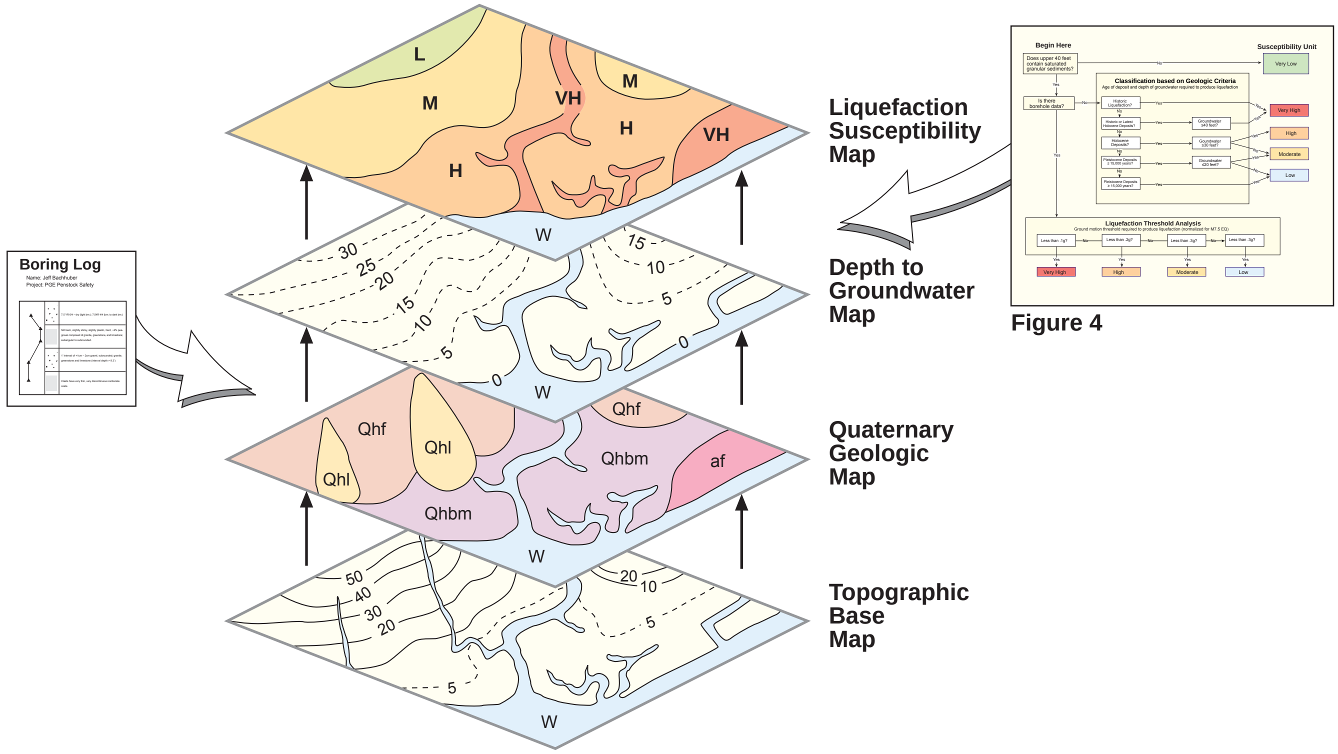

Figure 4a. Data sources and integration procedures to produce a liquefaction susceptibility map.

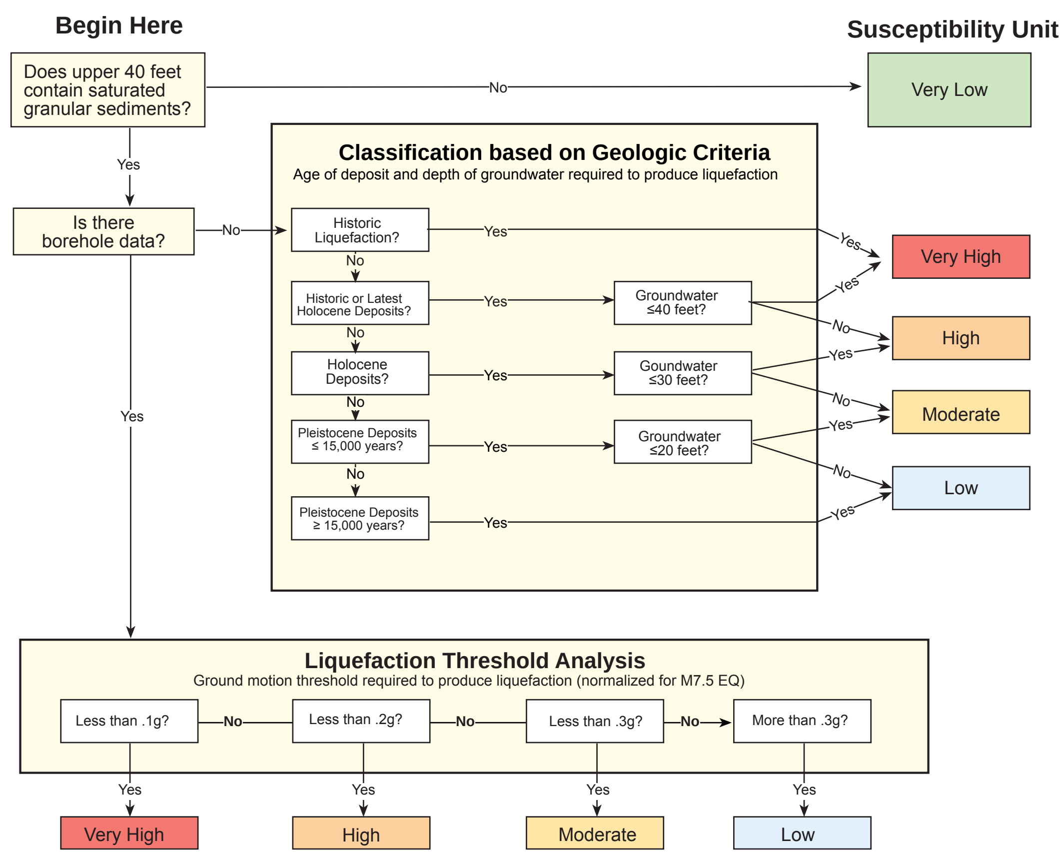

Figure 4b. Decision flow chart for evaluation of liquefaction susceptibility. Flow chart developed in cooperation with California Geological Survey for Simi Valley, California, with ground motion thresholds required to produce liquefaction normalized for a M7.5 earthquake (from Hitchcock et al., 1999).

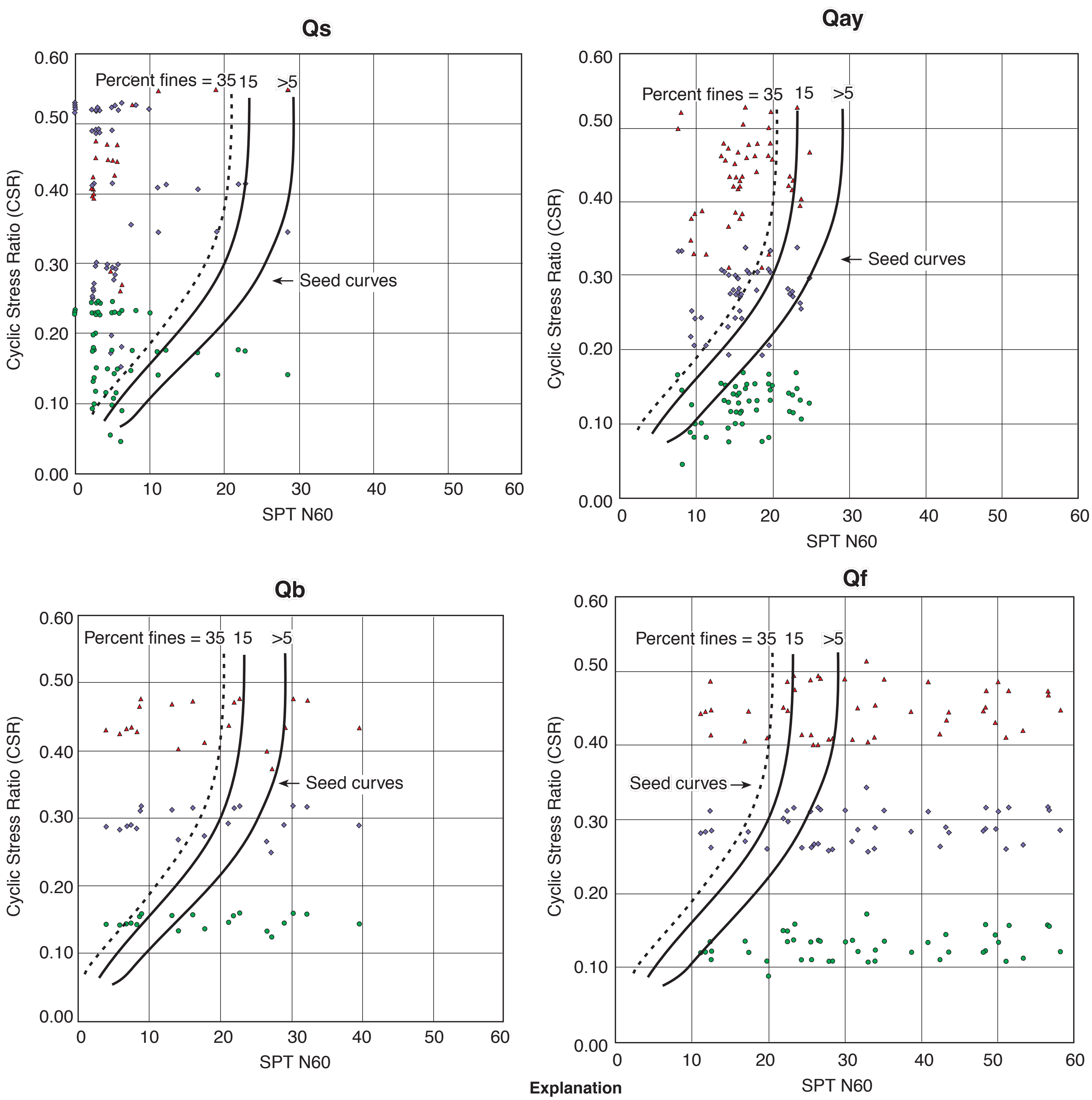

Explanation

SPT Blow Counts

- ◆ Cyclic stress ratio for 01.g peak ground acceleration (PGA)
- ● Cyclic stress ratio for 02.g peak ground acceleration (PGA)
- ▲ Cyclic stress ratio for 03.g peak ground acceleration (PGA)

Geologic Units

Qs	Holocene swamp deposits and overlying fill
Qb	Holocene beach deposits
Qay	Holocene alluvium
Qf	Late Pleistocene to early Holocene fan deposits

Note: CSR have been corrected for magnitude.

Figure 5a. Summary plots of Standard Penetration Test (SPT) blow count data versus cyclic stress ratio for various geologic units within San Juan Puerto Rico study area for a Magnitude M_W 7.5 earthquake. Potentially liquefiable sediments are indicated by blow count data that plot left of the Seed liquefaction triggering curves (modified from Seed and Idriss, 1971).

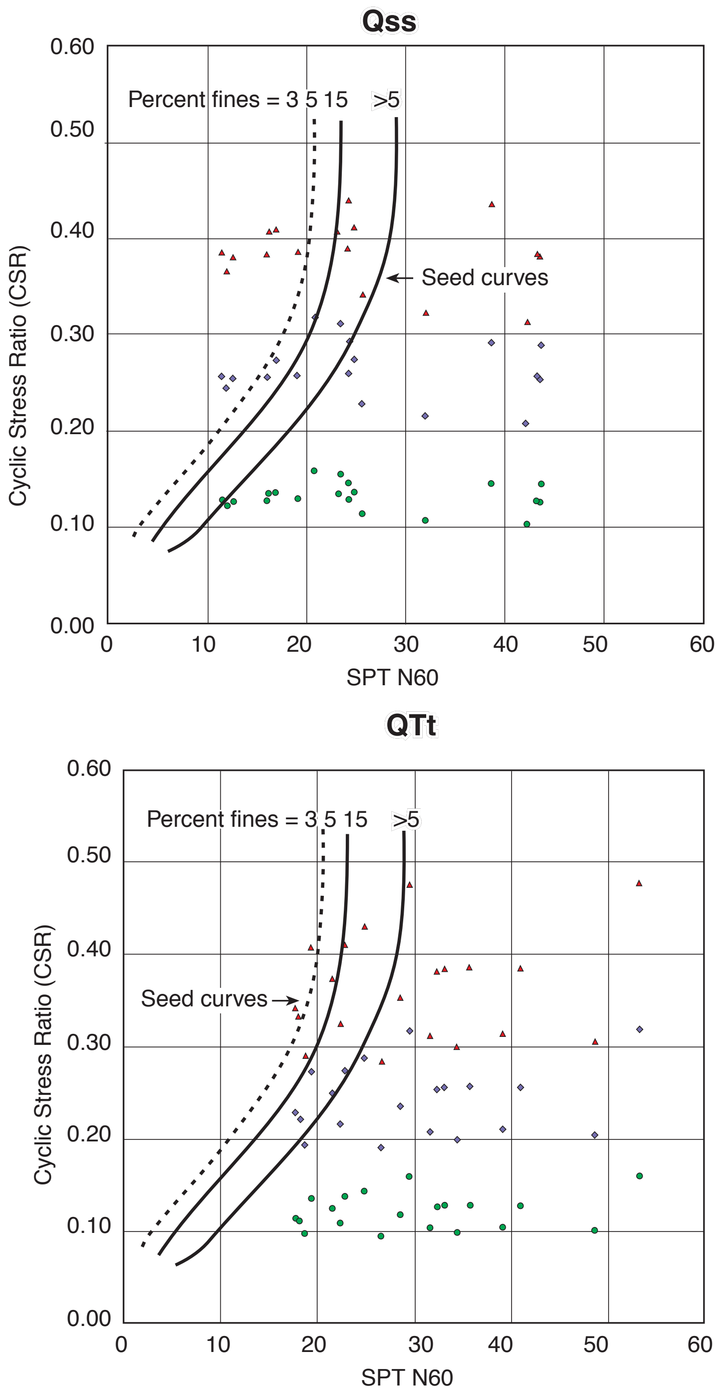

Note: CSR have been corrected for magnitude.

Explanation

SPT Blow Counts

- ◆ Cyclic stress ratio for 01.g peak ground acceleration (PGA)
- ● Cyclic stress ratio for 02.g peak ground acceleration (PGA)
- ▲ Cyclic stress ratio for 03.g peak ground acceleration (PGA)

Geologic Units

Qss Early Holocene to late Pleistocene (?) Santurce sands

QTt Pleistocene alluvium

Figure 5b.

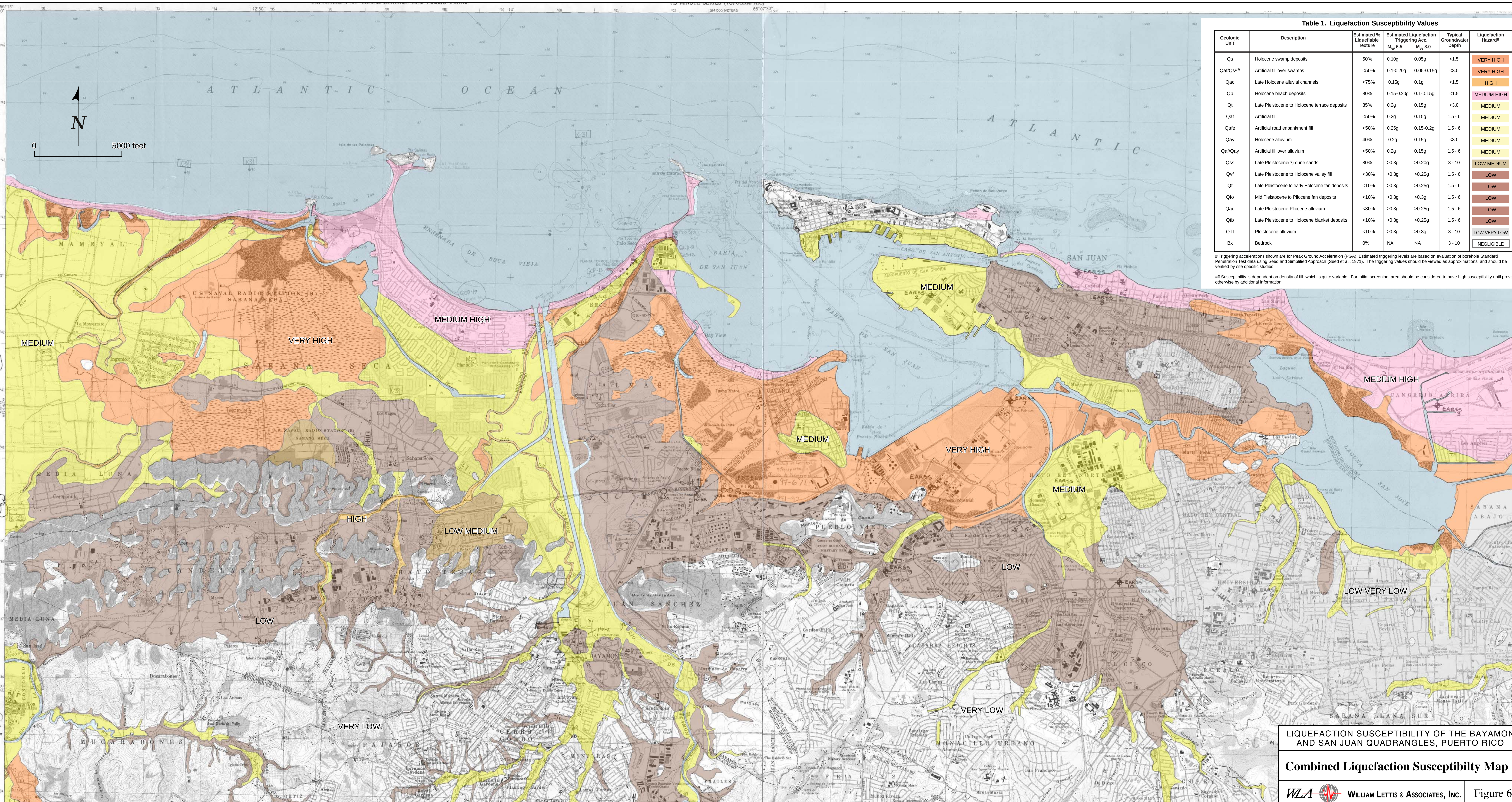

Table 1. Liquefaction Susceptibility Values

Geologic Unit	Description	Estimated % Liquefiable Texture	Estimated Liquefaction Triggering Acc. M_W 6.5	Estimated Liquefaction Triggering Acc. M_W 8.0	Typical Groundwater Depth	Liquefaction Hazard#
Qs	Holocene swamp deposits	50%	0.10g	0.05g	<1.5	VERY HIGH
Qaf/Qs##	Artificial fill over swamps	<50%	0.1-0.20g	0.05-0.15g	<3.0	VERY HIGH
Qac	Late Holocene alluvial channels	<75%	0.15g	0.1g	<1.5	HIGH
Qb	Holocene beach deposits	80%	0.15-0.20g	0.1-0.15g	<1.5	MEDIUM HIGH
Qt	Late Pleistocene to Holocene terrace deposits	35%	0.2g	0.15g	<3.0	MEDIUM
Qaf	Artificial fill	<50%	0.2g	0.15g	1.5 - 6	MEDIUM
Qafe	Artificial road enbankment fill	<50%	0.25g	0.15-0.2g	1.5 - 6	MEDIUM
Qay	Holocene alluvium	40%	0.2g	0.15g	<3.0	MEDIUM
Qaf/Qay	Artificial fill over alluvium	<50%	0.2g	0.15g	1.5 - 6	MEDIUM
Qss	Late Pleistocene(?) dune sands	80%	>0.3g	>0.20g	3 - 10	LOW MEDIUM
Qvf	Late Pleistocene to Holocene valley fill	<30%	>0.3g	>0.25g	1.5 - 6	LOW
Qf	Late Pleistocene to early Holocene fan deposits	<10%	>0.3g	>0.25g	1.5 - 6	LOW
Qfo	Mid Pleistocene to Pliocene fan deposits	<10%	>0.3g	>0.3g	1.5 - 6	LOW
Qao	Late Pleistocene-Pliocene alluvium	<30%	>0.3g	>0.25g	1.5 - 6	LOW
Qtb	Late Pleistocene to Holocene blanket deposits	<10%	>0.3g	>0.25g	1.5 - 6	LOW
QTt	Pleistocene alluvium	<10%	>0.3g	>0.3g	3 - 10	LOW VERY LOW
Bx	Bedrock	0%	NA	NA	3 - 10	NEGLIGIBLE

Triggering accelerations shown are for Peak Ground Acceleration (PGA). Estimated triggering levels are based on evaluation of borehole Standard Penetration Test data using Seed and Simplified Approach (Seed et al., 1971). The triggering values should be viewed as approximations, and should be verified by site specific studies.

Susceptibility is dependent on density of fill, which is quite variable. For initial screening, area should be considered to have high susceptibility until proven otherwise by additional information.

LIQUEFACTION SUSCEPTIBILITY OF THE BAYAMON AND SAN JUAN QUADRANGLES, PUERTO RICO

Combined Liquefaction Susceptibilty Map

WILLIAM LETTIS & ASSOCIATES, INC. Figure 6

01.23.08 1580 Bayamon NEHRP